ARTICLE IN PRESS

Optics Communications ▮ (▮▮▮▮) ▮▮▮–▮▮▮

Contents lists available at ScienceDirect

Optics Communications

journal homepage: www.elsevier.com/locate/optcom

Invited Paper

Transmission of multi-dimensional signals for next generation optical communication systems

Anlin Yi, Lianshan Yan *, Yan Pan, Lin Jiang, Zhiyu Chen, Wei Pan, Bin Luo

Center for Information Photonics & Communications, School of Information Science & Technology, Southwest Jiaotong University, Chengdu, Sichuan, 611756, China

ARTICLE INFO

Keywords:
Optical communication
Multi-dimension
Polarization-division-multiplexing (PDM)
Pseudo-PDM

ABSTRACT

Over the past several decades, the data-carrying capacity of a single optical fiber have been increased significantly by fully exploring and optimizing physical dimensions of the light. Generally there are five major candidates of dimensions, including time, wavelength, polarization, space and quadrature (phase and amplitude). Multi-dimension, utilizing more than two dimensions of the light simultaneously, is one of the essential characteristics of next generation optical communication systems. We review recent advances in transmission of multi-dimensional signals, and highlight innovative ways of exploring the polarization dimension to further increase the capacity or spectral efficiency of a single optical fiber, a so-called pseudo-polarization-division-multiplexing (PPDM) technique. Related demonstrations include non-orthogonal PDM, PPDM of three and four states (PPDM-3 and PPDM-4). Brief discussions on trends of multi-dimensional signal transmission technologies are also presented.

1. Introduction

With the rapid development of Internet-driven services, especially the explosive increases of the Internet-based video and peer-to-peer interactive applications, the global IP traffic broke the Zettabyte (ZB) threshold at the end of 2016 and it will grow at a compound annual growth rate (CAGR) of 22 percent from 2015 to 2020. By the end of 2020, global traffic will reach 2.3 ZB per year, or 194.4 EB per month under Cisco's forecast and methodology (Fig. 1) [1]. As a result, a global community of researchers and engineers is relentlessly striving to improve the backbone and local network infrastructures that can carry more data, more efficiently than ever before. Over the last several decades, optical communication technologies have been advancing rapidly, supporting the ever-growing bandwidth requirements. The transmission capacity of a single optical fiber now is up to 2.15 Pb/s [2]. To increase this figure-of-merit, researchers have been striving to find innovative ways to explore and optimize the physical dimensions of optical light. As shown in Fig. 2, mainly five physical dimensions can be used for modulation and multiplexing to increase the capacity over optical fiber links, i.e. time, wavelength, polarization, space (multicore fiber, linearly polarized (LP) modes, orbital-angular momentum (OAM) and vector modes) and quadrature (phase and amplitude) [2–12]. Obviously, ***multi-dimension***, utilizing more than two dimensions of the light simultaneously to increase the overall capacity, is one of the essential characteristics of next generation optical communication systems.

In this paper, we first give a brief overview of recent advances in transmission of multi-dimensional signals for next generation optical communication systems, with an emphasis on optical time-division-multiplexing (OTDM), wavelength-division-multiplexing (WDM), space-division-multiplexing (SDM), quadrature modulation and polarization-division-multiplexing (PDM). In Section 3, we present recent advances of exploring polarization dimension to increase the transmission capacity over standard single-mode-fiber (SMF) links, including non-orthogonal PDM, pseudo-PDM (PPDM) of three and four polarization states (PPDM-3 and -4). In Section 4, before the summary, we will briefly discuss the trends and challenges of multi-dimensional signal transmission technologies.

2. Review of multi-dimensional signals transmission technologies

As shown in Fig. 2, five physical dimensions can be employed to carry optical signals: time, wavelength, space, quadrature and polarization. These dimensions can be utilized independently or simultaneously to increase the data-carry capacity of optical communication systems.

* Corresponding author.
E-mail address: lsyan@swjtu.edu.cn (L. Yan).

http://dx.doi.org/10.1016/j.optcom.2017.07.046
Received 6 May 2017; Received in revised form 3 July 2017; Accepted 16 July 2017
Available online xxxx
0030-4018/

Please cite this article in press as: A. Yi, et al., Transmission of multi-dimensional signals for next generation optical communication systems, Optics Communications (2017), http://dx.doi.org/10.1016/j.optcom.2017.07.046.

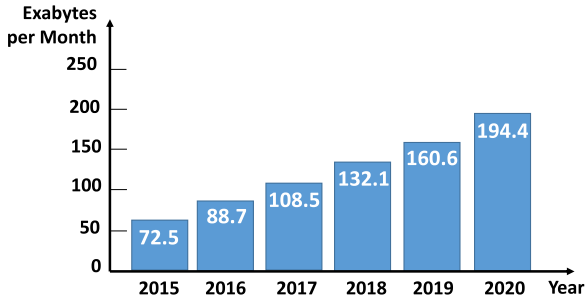

Fig. 1. Global IP traffic forecast and methodology (Source: Cisco VNI Ref. [1]).

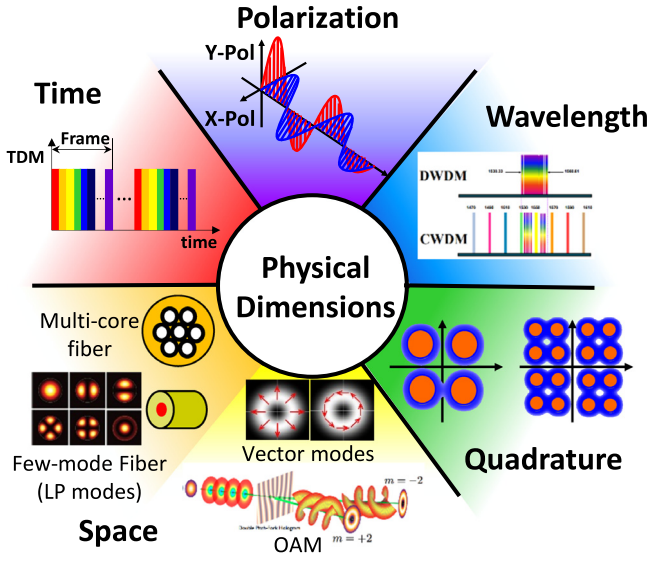

Fig. 2. Physical dimensions for optical communications.

2.1. Time dimension

The ***time dimension*** is exploited to increase the capacity over fiber by multiplexing signals in different bit slots in the time domain. In other words, it is practical to combine a set of low-bit-rate streams, each with a fixed and pre-defined bit rate, into a single high-speed bit stream that can be transmitted over fiber. This technique is well known as TDM. To optimize multiplexing in the time dimension, pulse shaping may be used to compress the spectrum of the temporal pulse subject to fundamental time-frequency constraints, and multi-level modulation formats may be employed to further increase bit-rate per pulse (e.g. PAM-4) [3,7]. TDM may be realized by electrical multiplexing (ETDM) or by optical multiplexing (OTDM) to a high-speed data signal [13–17]. Currently, almost all installed TDM optical communication systems are utilized ETDM. Experimental OTDM transmission was demonstrated as early as 1993 with bit rate of 100 Gb/s over 36 km fiber [15]. Since then, OTDM-transmission technologies have made a lot of advances toward much higher bit rates and much longer transmission links. 160 Gb/s transmission over a record length of 4320 km was reported in Ref. [16] and a record data rate of 2.56 Tb/s transmission over 160 km was reported in Ref. [17]. However, it is still a challenging task for OTDM technology to investigate the physical limits of ultra-high-speed and ultra-long haul fiber transmission and to search for appropriate and more practical techniques for data generation, transmission, and demultiplexing to extend these limits.

2.2. Wavelength dimension

Using the ***wavelength dimension***, one may multiplex a number of optical signals onto a single optical fiber by parallel using distinct wavelengths of the laser light, namely WDM in optical communications. In practical optical communication system, WDM technique, already an "inherited" one, usually combines with SDM, PDM, and quadrature modulation formats to increase the capacity of a single fiber. Additionally, to meet the bandwidth requirements, the capacity is increased by extending the WDM wavelength band from C-band to S-, L-, and U-band, as well as decreasing the channel space from 100 GHz to 50 GHz or even down to 25 GHz [9,18,19].

2.3. Space dimension

SDM, which utilizing the spatial dimension, refers to multiplexing techniques that establish multiple spatially distinguishable data paths through a single fiber. The SDM can be achieved by four ways, i.e. multi-core fiber (MCF), LP modes multiplexing using multi-mode-fiber (MMF), OAM and vector modes multiplexing. In the case of MCF, in which the distinguishable paths are defined by physically distinct single-mode cores (Fig. 2). The initial proposal of SDM using MCF were aimed at short-reach applications. *B. Rosinki* et al. firstly demonstrated 1 Gb/s data transmission over two cores of 4 core MCF at a wavelength of 850 nm [20]. Following greatly advances in the design and fabrication of single-mode MCF and related components (e.g. amplifier) [21–24], demonstrations of SDM transmission over MCF for long-haul applications have been showing impressive advances in terms of capacity, reach and spectral efficiency. Table 1 shows the mainly advances that have been made during the last few years. *H. Takara* and co-workers [25] firstly reported the Pb/s (1.01 Pb/s) capacity transmission experiment over 52 km 12 core MCF. Later, *H. Takahashi'* group demonstrated a long-haul (over 6160 km), WDM (40 × 103 Gb/s) transmission over MCF by firstly utilizing a multicore EDFA [26] and a record capacity-distance product of 1030.768 Pb/s × km was achieved [27]. *A. Turukhin* and co-workers transmitted a single wavelength and total capacity of 1.282 Tb/s 8D-APSK signal over the longest transmission distance over 14 350 km 12 core MCF by utilizing single mode EDFA [28]. *T. Mizuno* and co-workers reported a record 32 core long distance dense SDM (DSDM) transmission of over 1644.8 km using a crosstalk-managed transmission line [29]. Most recently, this group demonstrated the first 1 Pb/s DSDM unidirectional inline-amplified transmission experiment over 205.6 km of 32 core fiber using 100 GHz-spaced C-band WDM, utilizing a low crosstalk heterogeneous multi-core fiber [30].

MMF utilizes the linearly polarized modes to establish multiple spatially distinguishable data paths in a multi-mode fiber, which is well known as mode-division multiplexing (MDM). It is quite different from SDM transmission in MCF that the distinguishable mode paths have significant spatial overlap, and consequently signals are susceptible to coupling randomly among the modes during propagation [6–8]. To mitigate the crosstalk resulting from modes coupling during propagation, multiple-input multiple-out (MIMO) digital signal processing (DSP) techniques are needed at the receiver [31]. However, the DSP complexity requirements will increase rapidly with the multiplexed modes. Therefore, most significant MDM demonstrations have so far concentrated to few-mode fibers [32–42]. Table 2 shows the recent advances in MMF systems demonstrations. *R. Ryf* and co-workers transmitted 6 spatial modes and 32 WDM channels 16-QAM signals over 177 km FMF at spectral efficiency of 32 b/s/Hz [37], and 6 spatial modes and 32 WDM channels QPSK signals over 708 km FMF at a spectral-efficiency-distance product of 11 328 km × b/s/Hz [38]. A later, the longest transmission distance of 900 km for 32 WDM channels and 3 spatial modes with a 100 GHz channel spacing and a distance of 1500 km for a single wavelength channel 3 spatial modes experiment were achieved [39]. Most recently, the record of 15 spatial modes transmission over 23.8 km FMF was reported in Ref. [40]. The longest

Please cite this article in press as: A. Yi, et al., Transmission of multi-dimensional signals for next generation optical communication systems, Optics Communications (2017), http://dx.doi.org/10.1016/j.optcom.2017.07.046.

Table 1
Advances in MCF system demonstrations.

Year	Cores	Distance (km)	Format	Total capacity (Tb/s)	Capacity-distance product (Pb/s × km)	Ref.
2017	32	205.6	16-QAM	1000	205.6	[30]
2016	32	1644.8	16QAM	51.2	84.214	[29]
2016	12	14350	8D-APSK	1.282	18.391	[28]
2015	22	31	64-QAM	2150	66.65	[24]
2015	7	2520	QPSK	51.1	128.772	[23]
2014	7	7326	QPSK	140.7	1030.768	[27]
2013	7	6160	QPSK	28.8	177.408	[26]
2012	12	52	32QAM	1010	52.52	[25]

Table 2
Advances in MMF system demonstrations.

Year	Modes	Distance (km)	Format	Total capacity (Tb/s)	Capacity-distance product (Pb/s × km)	Ref.
2016	10	40	QPSK	0.4	0.016	[41]
2016	10	87	16QAM	67.5	5.873	[42]
2015	3	310	QPSK	18	5.58	[35]
2015	15	23.8	QPSK	18	0.428	[40]
2015	6	74.17	OFDM	41.6	3.085	[36]
2014	3	500	QPSK	33.288	16.644	[34]
2014	3	900	QPSK	9.6	8.64	[39]
2013	6	177	16QAM	24.6	4.354	[37]
2013	6	708	QPSK	6.1	4.319	[38]

transmission of 10 spatial modes over 40 km 50 μm core diameter MMF was demonstrated by *J. J. A. van Weerdenburg* and co-workers [41]. A record spectral efficiency of 58 b/s/Hz per fiber core was done by applying 30 GBaud 16-QAM over 87 km 10 modes FMF [42].

To further increase the transmission capacity, it is possible to combine the multicore and multimode approaches together [8]. The first experiments were carried out in Refs. [43,44]. DSDM transmission over the longest 527 km graded-index 12 core 3-spatial-mode fiber was been reported by *K. Shibahara's group* [45]. The record fiber capacity of 2.05 Pb/s and the highest aggregate spectral efficiency of 947 b/s/Hz DSDM transmission over 19 core 6-spatial-mode fiber were achieved by *D. Soma's* group successively [46].

OAM, sometimes described as the rotational analogue of linear momentum, is one of the most fundamental physical dimensions of laser light. It has given rise to many developments in optical manipulation, optical trapping, optical tweezers, optical vortex knots, imaging, astronomy, quantum information processing, and optical communication [10,57–61]. As for the application of optical communication areas, it typically uses OAM beams as information carriers for multiplexing that can be regarded as the analogue of WDM technique in optical fiber communications. The early demonstrations of OAM optical communication were focused on free-space information communication [10]. Until most recently, demonstrations of transmitting OAM signals in optical fiber have been reported, while over only several hundred meters or few kilometers [62–65]. In fibers, OAM beams are extremely unstable owing to strong mode coupling [62–65]. Therefore, it is a great challenge to investigate the physical limits for OAM signal transmission over long-haul optical fiber link and seek appropriate techniques to overcome these limits.

Vector modes are spatial modes that have spatially inhomogeneous states of polarization, such as radial and azimuthal polarization. The spatially inhomogeneous states of polarization of vector modes can be used for many applications, including optical trapping, nanoscale imaging, communications, and so on [11,12]. When using vector modes in communications, we can exploit either vector modes encoding scheme or vector modes multiplexing technique. *R. R. Alfana's* Group demonstrated an encoding scheme using four vector modes for optical communication [66]. Vector modes multiplexing technique for optical communication excites greatly interest lately as a new orthogonal multiplexing technique. 80 Gb/s vector modes multiplexing transmission QPSK signal over free space was carried out by *R. R. Alfana's* Group [67]. Most recently, 120 Gb/s vector modes multiplexing OFDM-32QAM and 95.16 Gb/s vector modes multiplexing OFDM-QSPK signal transmission in free space were achieved by *Z. Li's* group [68,69]. However, it is a great challenge to transmit vector modes signal in fiber as even the slightest perturbations to the cylindrical symmetry of fiber will induce strong coupling between the vector modes [70,71].

Although greatly advances have been made in SDM over the past years, much more work needs to be undertaken for improving the SDM systems performance competitive with those of existing single mode fiber systems.

2.4. Quadrature dimension

In communication systems, signal pulses are usually modulated onto the carrier wave whose frequency is much higher than the symbol rate. Ideal carrier wave is thought of having two independent components, sine and cosine, or real and imaginary, or in-phase and quadrature phase components, which are referred as the two ***quadrature dimensions***. Both quadrature dimensions can be exploited to modulate signal pulses resulting in two-dimensional symbols, such as quadrature-amplitude-modulation (QAM) shown in Fig. 2 (quadrature parts) [7,9]. Modulation signal pulses onto two quadrature dimensions of the carrier wave was initially exploited in wireless communication systems whose carrier wave frequency is much lower than optical carrier frequencies. Following the greatly advances in the design and fabrication of optical components (e.g. laser, optical modulator, optical hybrid and so on) and coherent detection techniques, modulation signal pulses onto two quadrature dimensions of the optical carrier wave have been developed impressively [47–56]. Multi-level QAM signal is becoming an attractive way to increase the fiber capacity. Table 3 summarizes the most recent productive demonstrations of quadrature modulation formats transmission for long-haul optical communication systems. 2048-QAM single-carrier transmission over 150 km single mode fiber with 66 Gb/s capacity was realized by *S. Beppu* and co-workers [53]. Total capacity of 52.2 Tb/s 16-QAM signal transmission over the longest distance of 10 230 km SMF was reported by *J. X. Cai'* group [54], and them demonstrated transmission of total capacity up to 63.5 Tb/s over 5380 km SMF using the 64-QAM later [55]. The record total capacity-distance product of about 226.4 Pb/s × km over 6800 km SMF using 32-QAM was achieved by *S. L. Zhang's* group [56]. Generally, the capacity can be increased by raising the modulation level of QAM signal under the same Baud rate. However, the higher level QAM signals are more susceptible to system parameters (e.g. laser linewidth, fiber nonlinearity), resulting the carrier-phase estimation algorithm becoming complex and degrading the system performance. Therefore, it is better to make well

Please cite this article in press as: A. Yi, et al., Transmission of multi-dimensional signals for next generation optical communication systems, Optics Communications (2017), http://dx.doi.org/10.1016/j.optcom.2017.07.046.

Table 3
Advances in quadrature dimensions.

Year	Modulation Format	Distance (km)	Capacity per λ (Gb/s)	Total Capacity (Gb/s)	Capacity-distance product (Tb/s× km)	Ref.
2015	2048-QAM	150	66	66	9.9	[53]
2017	512-QAM	160	216	216	34.56	[47]
2016	256-QAM	160	320	320	51.2	[48]
2017	128-QAM	80	400	12000	960	[49]
2017	64-QAM	300	1000	1000	300	[50]
2015	64-QAM	5380	233.5	63500	341630	[55]
2016	32-QAM	6800	198.2	33300	226423.68	[56]
2015	32-QAM	660	1000	1000	660	[51]
2014	16-QAM	10230	192	52200	534000	[54]
2016	QPSK	7878	400	3600	28360.8	[52]

trade-offs among the modulation level, capacity, distance and spectral efficiency in long-haul, ultra-high speed and high spectral efficiency optical communication systems.

2.5. Polarization dimension

The polarization of light, as another one of the most fundamental physical dimensions in classical and quantum mechanics, can be exploited to simultaneously transmit independent signals on a set of polarizations. PDM carries two independent signals at the same wavelength with two orthogonal polarizations. It can double the system capacity and spectral efficiency directly compared with single-polarization systems [72–75]. Similar to other dimensions, it can also combine with the information coded in quadrature dimension techniques (e.g. QAM formats) to increase the capacity. Actually, the scheme that incorporates quadrature modulation formats and PDM, as well as WDM, has become one of the most practical techniques in ultra-high-speed optical communication systems [76–79]. However, multiplexing of polarizations, as an independent dimension of freedom, is still limited to orthogonal state of polarizations (SOPs) in PDM systems. It would be highly desirable if the orthogonality of polarization could be broken to enable the signal to accommodate more polarization states at a single wavelength, similar to WDM or SDM. Multiplexing of more than two conventional SOPs was reported as long ago as 1986, when it was only implemented in the free-space [80]. Recently, focus has turned to the construction of novel communication systems through additional polarization manipulation [81,82]. Due to certain physical limitations, only on-off-keying (OOK) signal transmissions have been achieved either theoretically or experimentally. Among these, Ref. [82] describes the first experimental attempt of quad-polarization transmission, in which four SOPs are carried by four individual wavelengths and the transmission distance is limited to only 2 km. Therefore, the feasibility of improving spectral efficiency (i.e., quadrupling or improving by even larger factors), using advanced modulation formats (e.g., phase-shift-keying), and transmitting over longer distance by polarization manipulation is still questionable. In Section 3 of this paper, the most recent developments of innovation ways for manipulation polarization states will be discussed in details.

3. Multiplexing and demultiplexing of multiple polarization states

As mentioned before, it would be highly desirable if the orthogonality of polarization could be broken to enable the signal to accommodate more polarization states at a single wavelength. Apparently the first change to face is to find the way to optimize the transmission performance of two polarization states that are not orthogonal any more.

One of the most popular methods of polarization demultiplexing for PDM signals, especially for complex modulated signals, is to utilize the Stokes vector in the Poincaré sphere. The signal described by the Stokes vector is independent of linewidth, frequency offset, and pulse shaping. Illustrations of unconventional and conventional polarization-multiplexed schemes in the relative distribution and the Stokes space are shown in Fig. 3. The left column shows the DPSK signals multiplexed with non-orthogonal polarizations, three polarizations and four polarizations (Fig. 3a). For comparison, we also illustrate the conventional PDM strategy for three different standard modulation formats: DPSK, QPSK, and 8-quadrature amplitude modulation (8-QAM, Fig. 3b). As can be observed from the relative distribution of the signal, in which the phase evolution is denoted by color shading, great differences exist between unconventional and conventional polarization-multiplexing. However, in the Stokes space, the distribution and trajectory (circles in Fig. 3) of the Stokes vector for both multiplexing strategies are similar. Therefore, similar to the polarization demultiplexing of PDM-QPSK and PDM-8QAM, PPDM-3 or -4 DPSK could be demultiplexed as well based on Stokes analysis. The demultiplexing of multiple polarization states can be divided into two steps: 1) polarization alignment (i.e. polarization tracking) and 2) demapping. Similar to Ref. [83], the polarization alignment is implemented in Stokes space. The key of the polarization alignment is to establish the fitted line (i.e. Non-orthogonal system) or plane (i.e. PPDM-3 and -4 DPSK), and to find the normal $\boldsymbol{n}$ (i.e. $[n_1, n_2, n_3]$) of the fitted line or plane. Then, the inverse transformation matrix M^{-1} can be calculated by $\boldsymbol{n}$, and expressed as:

$$M^{-1} = \begin{pmatrix} \cos(\alpha)\exp(j\Delta\phi/2) & \sin(\alpha)\exp(-j\Delta\phi/2) \\ -\sin(\alpha)\exp(j\Delta\phi/2) & \cos(\alpha)\exp(-j\Delta\phi/2) \end{pmatrix} \quad (1)$$

where $\alpha = 1/2\text{atan}\left(\sqrt{n_2^2+n_3^2}, n_1\right) - \theta$, and $\Delta\phi = \text{atan}\left(n_3, n_2\right)$. In this case, the polarization alignment can be successfully achieved, and the demapping of non-orthogonal, PPDM-3 and PPDM-4 system is presented in the following, respectively.

3.1. Non-orthogonal polarization multiplexing

Up to now, there are some notable works about the minimum polarization multiplexing angle (e.g. 45° and 60°) in PDM systems [80,82] while the transmission distance is limited to only a few kilometers. Here, an innovative way of exploring the minimization of polarization multiplexing angle (i.e. $\theta = 23°$,) with long-reach transmission (i.e. 400 km SMF) for DPSK modulation format is introduced [84].

The detailed operation principle of the proposed algorithm for demultiplexing the non-orthogonal polarization states (e.g. p_1 and p_2) with the polarization multiplexing angle θ that is less than 90° is described as following. The Jones vector representing the received optical wave shown as Figs. 4 (a-i) with non-orthogonal polarization states can be written:

$$E = \frac{1}{\sqrt{2}}\begin{pmatrix} e_x \\ e_y \end{pmatrix} = \frac{1}{\sqrt{2}}\begin{pmatrix} [\cos(\alpha)+\cos(\theta+\alpha)]\exp\left(jwt+j\phi_x\right) \\ [\sin(\alpha)+\sin(\theta+\alpha)]\exp\left(jwt+j\phi_y\right) \end{pmatrix}, \quad (2)$$

where θ and α are the polarization multiplexing angle and the rotation angle, respectively. The multiplier $1/\sqrt{2}$ is required for normalization. The Jones vector E of Eq. (2) is transformed into the Stokes vector. The components of Stokes vector can be derived further as

$$s_0 = \left(|e_x|^2 + |e_y|^2\right)/2 = 1 + \cos(\theta), \quad (3)$$

$$s_1 = \left(|e_x|^2 - |e_y|^2\right)/2 = \cos(\theta+2\alpha)[1+\cos(\theta)], \quad (4)$$

$$s_2 = |e_x||e_y|\cos\Delta\phi = \{\sin(\theta+2\alpha)[1+\cos(\theta)]\}\cos\Delta\phi, \quad (5)$$

$$s_3 = |e_x||e_y| sin\Delta\phi = \{\sin(\theta+2\alpha)[1+\cos(\theta)]\} sin\Delta\phi \quad (6)$$

Please cite this article in press as: A. Yi, et al., Transmission of multi-dimensional signals for next generation optical communication systems, Optics Communications (2017), http://dx.doi.org/10.1016/j.optcom.2017.07.046.

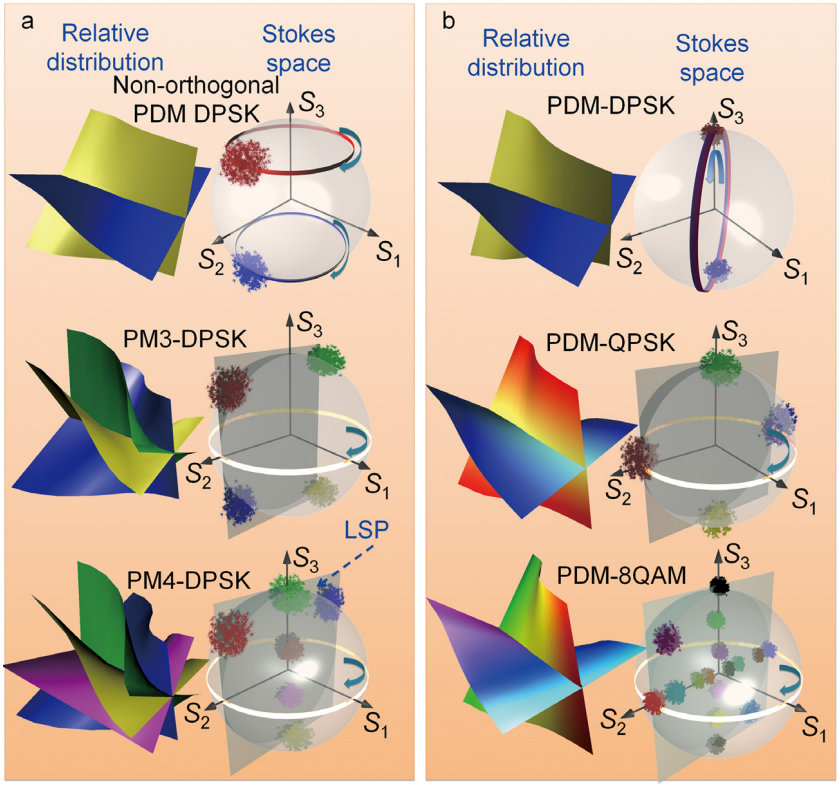

Fig. 3. Illustration of unconventional and conventional polarization-multiplexed schemes in relative distribution and the Stokes space. (a) DPSK signal multiplexing with two non-orthogonal polarizations, three polarizations and four polarizations. (b) Conventional polarization-multiplexed schemes of three different standard modulation formats including PDM-DPSK, PDM-QPSK and PDM-8QAM. LSP: least squares plane.

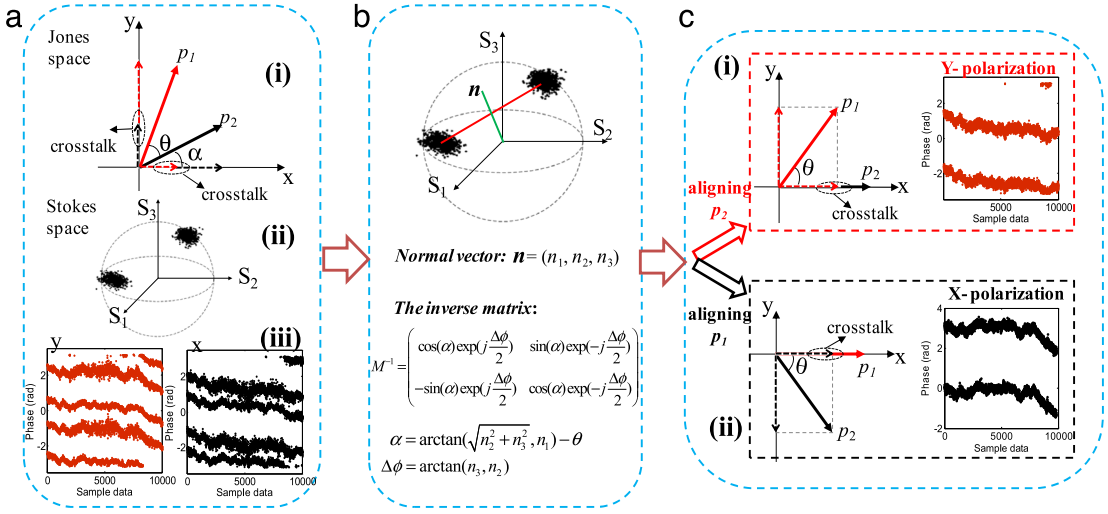

Fig. 4. The minimization of polarization multiplexing angle in PDM systems for DPSK modulation format: (a) before polarization demultiplexing; (b) the proposed demultiplexing scheme; (c) after polarization demultiplexing.

where $\Delta\phi = \phi_x - \phi_y$ is the phase difference between the received x and y polarization components. Here, the frequency offset between the signal and the local oscillator is neglected. The first component of the Stokes parameters s_0 represents the total signal power, and the remaining three components s_1, s_2, s_3 represent 0° linear, 45° linear and circularly polarization component, respectively. Therefore, the received optical wave (polarization multiplexed signals) can be finally mapped into the Stokes space (as shown in Figs. 4(a-ii) or Fig. 4(b)). If the two polarization tributaries are not exactly orthogonal (i.e. when they are orthogonal, two polarization tributaries is 90° in Jones space, 180° in Stokes space), the two Stokes constellation points is separated by $90° + 2\theta$. It is worth noting that only one of the polarization tributaries (e.g. p_1) is demultiplexed perfectly (without crosstalk) if the rotation angle α is used in Eq. (1), while the other polarization tributary (i.e. p_2) is yet inherited with crosstalk. Therefore, to perfectly demultiplex p_2, we can replace the rotation angles α with $\alpha - \theta$ in Eq. (1). Subsequently the two polarization tributaries could be simultaneously demultiplexed by using the rotation angles α and $\alpha - \theta$ in Eq. (1), respectively (as shown Fig. 4(c)). To sum up, the demultiplexing process is to respectively align different principal polarization axes.

The bit-error-rate (BER) results in Fig. 5(a) show that the proposed scheme can successfully demultiplex the 56 Gb/s PDM-DPSK signals with different polarization multiplexing angles (i.e. θ = 23°, 45°, 67°).

Please cite this article in press as: A. Yi, et al., Transmission of multi-dimensional signals for next generation optical communication systems, Optics Communications (2017), http://dx.doi.org/10.1016/j.optcom.2017.07.046.

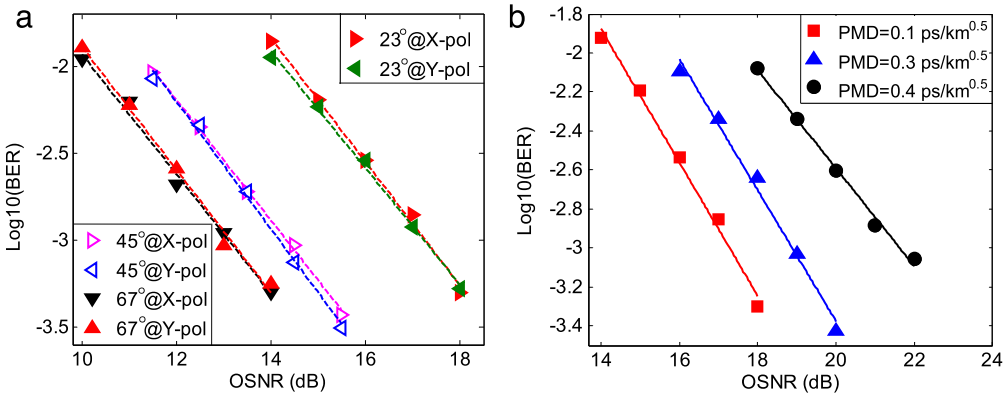

Fig. 5. 56 Gb/s PDM-DPSK transmission over 400 km: (a) BER performance for different polarization multiplexing angles (i.e. θ = 23°, 45°, 67°); (b) BER performance for different PMD values (i.e. PMD = 0.1, 0.3, 0.4 ps/km 0.5) with the multiplexing angle of 23°.

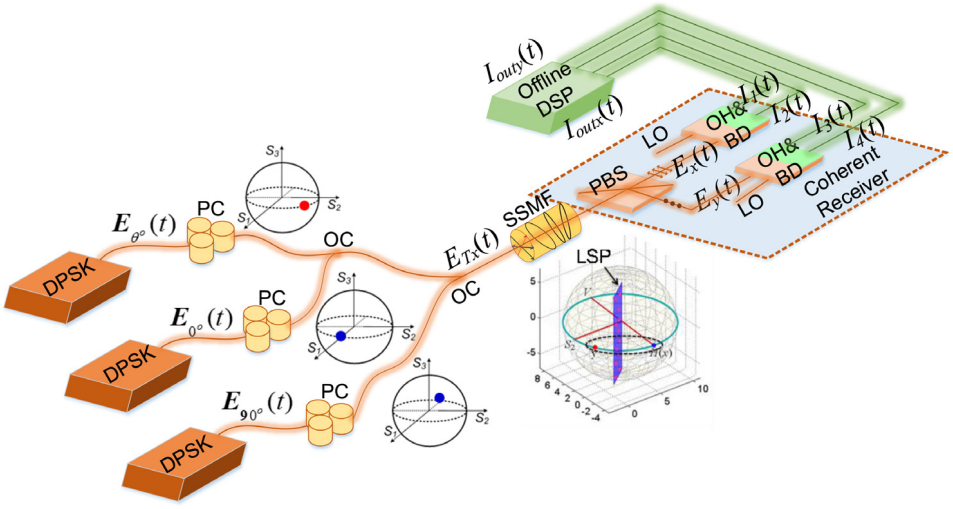

Fig. 6. Schematic diagram of the PPDM-3 DPSK signal. PC: polarization controller; OC: optical coupler; SSMF: standard single mode fiber; PBS: polarization beam splitter; LO: local oscillator; OH: 90° optical hybrid; BD: balanced detector; DSP: digital signal processing.

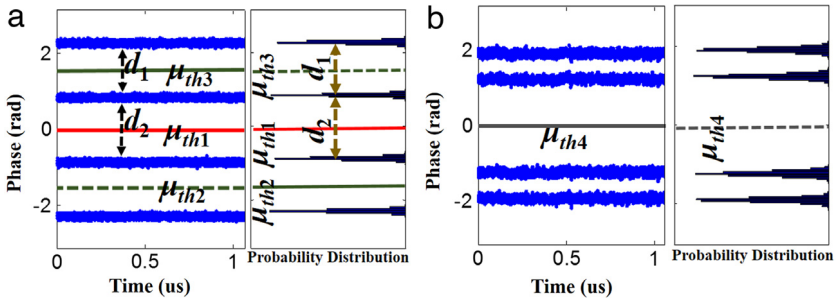

Fig. 7. Simulated phase information of (a) *x*-axis and (b) *y*-axis received signals after phase drift compensation.

The comparison of optical signal-to-noise-ratio (OSNR) penalties between different polarization multiplexing angles indicates that smaller multiplexing angle corresponds to more severe crosstalk in the receiver side. Since polarization-mode-dispersion (PMD) may also bring about crosstalk, we further investigate the demultiplexing performance when the transmission fiber link has certain amount of PMD. Fig. 5(b) shows the BER performance for different PMD values (i.e. PMD = 0.1, 0.3 and 0.4 ps/km$^{0.5}$) with the multiplexing angle of 23°. As expected, the non-orthogonal polarization multiplexed signals are more susceptible to the link PMD that results in severe crosstalk between two polarization tributaries. As shown in Fig. 5(b), the relative OSNR penalty at 10^{-3}BER for the PMD values of 0.1 and 0.4 ps/km$^{0.5}$ is ~ 4 dB. The OSNR penalty would increase more rapidly when the mean differential-group-delay (DGD) becomes larger. It is mainly because that the polarization crosstalk would have a strong impact on the performance of PDM system with multiplexing angle 23°. Therefore, PMD compensation method in either time or frequency domain would be desired to further improve the demultiplexing performance.

3.2. Pseudo-PDM of three states (PPDM-3)

When more than two polarization states are used for multiplexing, as they are not orthogonal to each other, we call it as pseudo-PDM (PPDM). Fig. 6 illustrates the principle of the multiplexing and demultiplexing

Please cite this article in press as: A. Yi, et al., Transmission of multi-dimensional signals for next generation optical communication systems, Optics Communications (2017), http://dx.doi.org/10.1016/j.optcom.2017.07.046.

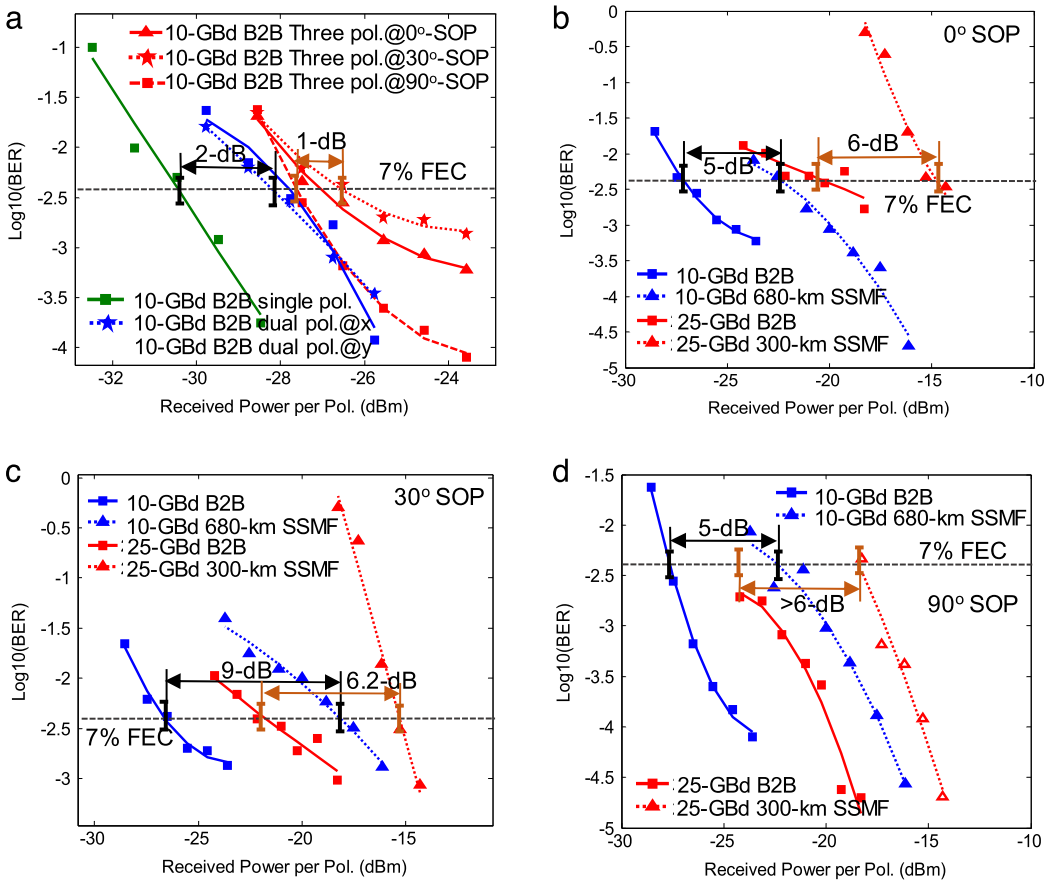

Fig. 8. Measured BER versus received optical power (per polarization) for back-to-back and transmission configurations: (a) back-to-back performance of single, dual and three polarization multiplexing system. The BER performances for (b) 0°-SOP, (c) 30°-SOP and (d) 90°-SOP. Pol.: Polarization.

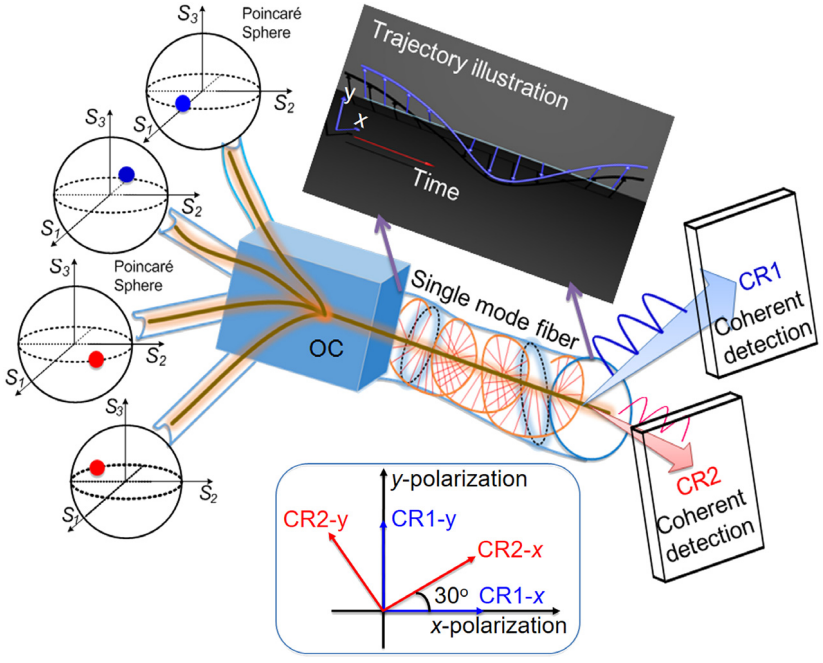

Fig. 9. Conceptual illustration of PPDM-4 DPSK system for long-haul transmission; CR: coherent receiver. Insets illustrate the typical trajectory of PPDM signal transmission in the fiber and the relationship of four principal axes of two coherent receivers.

for PPDM of three polarization states (PPDM-3) that carry DPSK signals (i.e. the multiplexing angles are 0°, θ° and 90°) [85]. Three independent DPSK signals with difference states of polarization (SOPs) are multiplexed by the polarization controllers (i.e. PCs) and optical couplers

Please cite this article in press as: A. Yi, et al., Transmission of multi-dimensional signals for next generation optical communication systems, Optics Communications (2017), http://dx.doi.org/10.1016/j.optcom.2017.07.046.

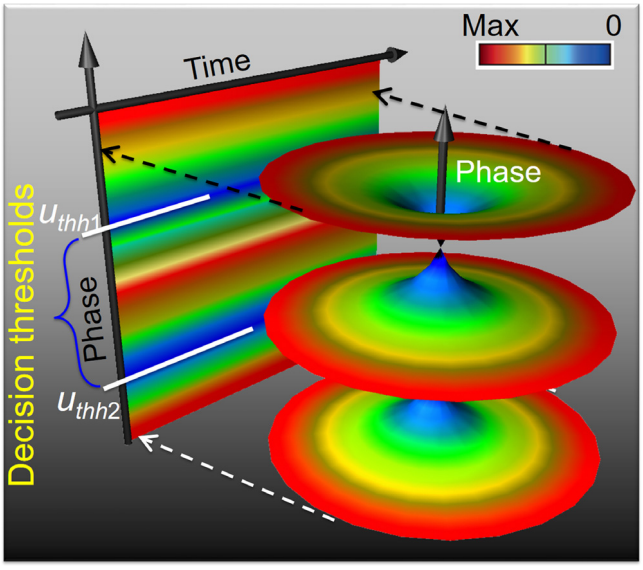

Fig. 10. The phase density diagram for determining the decision thresholds when 0° SOP aligned to a principal axis of CR1.

(OCs). After transmission over the standard SMF (SSMF), the PPDM-3DPSK signal is injected into a coherent receiver. Along the principal axis of the receiver (i.e. x- and y-axis), the input optical signal can be divided into horizontal component $E_x(t)$ and vertical component $E_y(t)$. We assume that the SOPs of 0° and 90° are aligned to x- and y-axis, respectively. After 90° optical hybrid and balanced detector, the electrical signals are achieved as

$$\begin{aligned} I_{outx}(t) &= I_1(t) + j \times I_2(t) = a(t) \times \exp\left\{j \times \left[\varphi_{0^\circ}(t) + \varphi'_{n0^\circ}(t) - \pi/2\right]\right\} \\ &\quad + [b(t) \times \cos(\theta)] \times \exp\left\{-j \times \left[\varphi_{\theta^\circ}(t) + \varphi'_{n\theta^\circ}(t)\right]\right\}, \\ I_{outy}(t) &= I_3(t) + j \times I_4(t) = c(t) \times \exp\left\{j \times \left[\varphi_{90^\circ}(t) + \varphi'_{n90^\circ}(t) - \pi/2\right]\right\} \\ &\quad + [d(t) \times \sin(\theta)] \times \exp\left\{-j \times \left[\varphi_{\theta^\circ}(t) + \varphi'_{nn\theta^\circ}(t)\right]\right\} \end{aligned} \tag{7}$$

where $a(t)$, $b(t)$, $c(t)$ and $d(t)$ are the coefficients that determined by optical power and fiber effects, $\varphi_{0^\circ,\theta^\circ,90^\circ}(t)$ and $\varphi'_{n0^\circ,n\theta^\circ,n90^\circ,nn\theta^\circ}(t)$ are the modulated phase and phase noises of the 0°, θ° and 90° SOP, respectively.

As seen from Eq. (7), the signals after optical detection may suffer from severe crosstalk and it is hardly demultiplexed directly. However, if the phase noise is compensated for $I_{outx}(t)$ and $I_{outy}(t)$, the phase of the signal can be calculated, which leads to the polarization demultiplexing method more easy. To simplify the discussion, a simulation of PPDM-3 transmission is performed assuming that the symbol rate, laser linewidth and θ are 10 GBaud, 100 kHz, and 30°, respectively. When the polarization is well aligned, the simulated phase information of received signals after phase noise compensation are shown in Fig. 7, where the decision thresholds $\mu_{th1} \sim \mu_{th4}$ are presented according to the statistical histograms of phase density for different polarization tributaries. In this case, four thresholds $\mu_{th1} \sim \mu_{th4}$ can be obtained obviously when the density of phase is lowest. According to the phase distribution, we can make a distinction between 0°-SOP and 30°-SOP by introducing the distances between two neighboring phase levels d_1 and d_2. According to Eq. (7), d_1 and d_2 can be expressed as $2\times arctan\{a(t)/[b(t) \times \cos(\theta^\circ)]\}$ and $2\times arctan\{[b(t) \times \cos(\theta^\circ)]/a(t)\}$, respectively. If $d_1 < d_2$, 0°-SOP tributary is in the low level when $\phi_{outx} < \mu_{th1}$, otherwise, it is in the high level. Meanwhile, 30°-SOP tributary is in the low level when $\mu_{th2} < \phi_{outx} < \mu_{th3}$, otherwise, it is in the high level. If $d_1 > d_2$, 0°-SOP is in the low level when $\mu_{th2} < \phi_{outx} < \mu_{th3}$, otherwise, it is in the high level. On the other hand, 30°-SOP is in the low level when $\phi_{outx} < \mu_{th1}$, otherwise, it is in the high level. Correspondingly, the 90°-SOP tributary is determined to be low level when $\phi_{outy} < \mu_{th4}$, while it is in the high level when $\phi_{outy} \geq \mu_{th4}$.

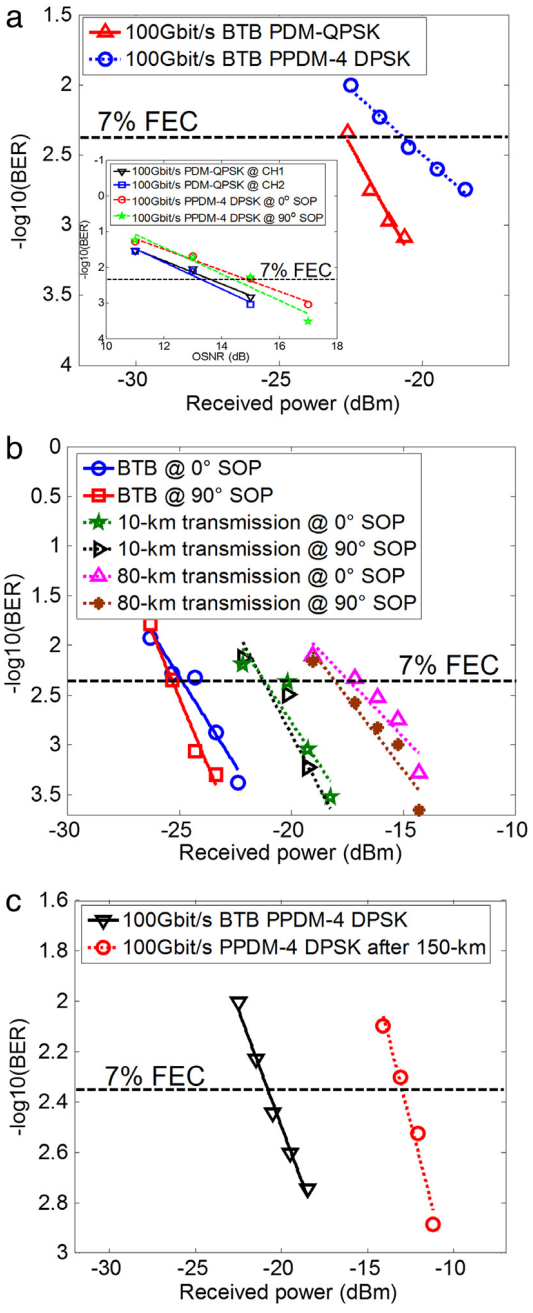

Fig. 11. Measured BER performances; (a) shows the performance comparison between PPDM-4 DPSK system and PDM-QPSK system under the same SE and the same bit rate (100 Gb/s). Inset illustrates the simulation results; (b) shows the back-to-back, 10 km transmission and 80 km transmission bit-error-rate performances for 40 Gb/s DPSK signal; (c) shows the back-to-back and 150 km transmission performances for 100 Gb/s PPDM-4 DPSK signal.

Fig. 8(a) shows the back-to-back performance of single, dual and three polarization multiplexing system (i.e. the multiplexing angles are 0°, 30° and 90°) at the rate of 10 GBaud for a comparison. As shown in Fig. 8(a), the power penalty of the proposed scheme is about 2.5 dB for 0°-SOP and 90°-SOP at 7% FEC limit compared to the single polarization system, and about 3.5 dB penalty for the 30°-SOP case. Compared to the orthogonal polarization-division-multiplexed (PDM) system, the power penalties of the proposed scheme are negligible for 0°-SOP and 90°-SOP, and 1 dB for 30°-SOP is observed. Figs. 8(b), (c) and (d) show the BER performances versus input power before the receiver for 0°-, 30°- and 90°-SOP, respectively. Approximately 5 dB power penalty is

Please cite this article in press as: A. Yi, et al., Transmission of multi-dimensional signals for next generation optical communication systems, Optics Communications (2017), http://dx.doi.org/10.1016/j.optcom.2017.07.046.

observed at 7% FEC limit when the multiplexed signal transmits over 680 km at 3 × 10 Gb/s for 0°-SOP. Afterwards, the rate of signal is increased to 3 × 25 Gb/s, and the transmission distance is reduced to 300 km. The power penalty increases to 6 dB at 7% FEC correspondingly. Meanwhile, the power penalty is about 9 dB after transmission over 680-km at 3 × 10 Gb/s and about 6.2 dB after transmission over 300 km at rate up to 3 × 25 Gbit/s for 30°-SOP. For the tributary of 90°-SOP, the power penalties are about 5 dB and >6 dB after 680 km and 300 km transmission, respectively.

3.3. Pseudo-PDM of four polarization states (PPDM-4)

Fig. 9 illustrates the multiplexing and demultiplexing scheme for the PPDM-4 transmission of DPSK signals [5]. The setup is similar to that of PPDM-3. Assuming that the SOPs of the four states are 0°, 30°, 90° and 120°. The multiplexed signal is subsequently transmitted over SMF with varying polarization, whose typical trajectory is illustrated in the inset of Fig. 9. At the receiver side, the PPDM-4 DPSK signal is first split into two streams (i.e., E_1 and E_2) by an OC. Subsequently, two coherent receivers (CR1 & CR2) are employed to detect the signal and extract the Stokes vector **S**. Taking CR1 as an example, when 0° SOP aligned to a principal axis of CR1, a novel visual illustration termed the phase density diagram is provided to determine the decision thresholds as shown in Fig. 10, where color denotes the density of the signal phases. Typically, the phase density of PPDM-4 DPSK is divided into three levels at any time point. Between these levels, two decision thresholds (i.e., u_{thh1} & u_{thh2}) for the E_{1x} tributary that correspond to the low-density regions can be determined. The 2D diagram of Fig. 10 shows the decision thresholds more clearly according to the values of the blue points. Finally, the 0° polarization tributary (or 90° polarization tributary) is determined to be at a low level when $u_{thh2} \le u_h \le u_{thh1}$ (or $u_{thv2} \le u_v \le u_{thv1}$), where u_h and u_v are the two tributaries after phase recovery. The parameters u_{thhi} and u_{thvi} (i = 1 and 2) are decision thresholds for 0° polarization and 90° polarization, respectively. Otherwise, they are at a high level. For the other two channels (i.e., 30° polarization and 120° polarization), the demodulation algorithm is the same as in the previous process.

The back-to-back BER performance of a 4 × 25 Gb/s PPDM-4 DPSK system is compared to that of a 100 Gb/s PDM-QPSK signal under the same spectral efficiency as shown in Fig. 11(a). It can be observed that the power penalty is approximately 2 dB at the 7% FEC threshold. This finding indicates that the proposed scheme can be used as an alternative to PDM-QPSK in a flexible-rate coherent system, demonstrating the potential of using the freedom of polarization for future optical networks to further increase the system capacity and spectral efficiency without changing current devices or system infrastructures. The BER under different transmission rates and different transmission lengths are also compared as shown in Fig. 11(b). Here, only tributaries of 0° polarization and 90° polarization are presented since the performance of the other two channels (i.e., 30° polarization and 120° polarization) is similar to these two tributaries. When the transmission rate decreases to 40 Gb/s, the back-to-back receiver sensitivities of 0° polarization and 90° polarization are −25.3 dB and −24.9 dB, respectively. Subsequently, when the PPDM-4 DPSK signal is fed into the 10 km and 80 km SMF, the receiver sensitivities at 7% FEC are −21.24 dB, −21.19 dB, −18.04 dB and −17.41 dB for 0° polarization and 90° polarization. Finally, the BTB and transmission performances of a 100 Gb/s PPDM-4 DPSK signal is also investigated as shown in Fig. 11(c). A transmission distance of up to 150 km is realized with a power penalty of 8 dB. While we have to admit that there are certain challenges need to be overcame when the multi-level signals (i.e. M-PSK and M-QAM) are applied to the pseudo-PDM schemes, including phase drift compensation, polarization crosstalk management, instable phase relationship, and so on. It is expected though that multi-level signals over multiple polarization-multiplexed systems could be accomplished after these challenges being solved in the near future.

4. Discussions & Conclusion

Great advances has been made in multi-dimension signal transmission over the past several decades. Various innovative technological approaches have been developed, which significantly improve the overall capacity of a single optical fiber, as well as other figure-of-merits, such as reach, spectral efficiency and capacity-distance product. However, much more efforts need to be spent to optimize these approaches from the practical point of view and make system performance competitive with those of existing systems in terms of cost, reliability, operability and so on. As the growth of bandwidth requirements is endless, investigating the physical dimension limits for multi-dimension signal transmission over long-haul optical communication systems and seeking appropriate techniques to further breakthrough those limits are still a great challenge in future.

Acknowledgment

This research is supported by the Natural Science Foundation of China (No. 61335005, 61325023, 61401378).

References

[1] Cisco visual networking index: Cisco VNI forecast and methodology, 2015~2020 White Paper. http://www.cisco.com/c/en/us/solutions/collateral/service-provider/visual-networking-index-vni/complete-white-paper-c11-481360.html.
[2] B.J. Puttnam, R.S. Luís, W. Klaus, J. Sakaguchi, J.M. Delgado Mendinueta, Y. Awaji, N. Wada, Yoshiaki Tamura, Tetsuya Hayashi, Masaaki Hirano, J. Marciante, 2.15 Pb/s Transmission using a 22 core homogeneous single-mode multi-core fiber and wideband optical comb, in Proceedings of European Conference and Exhibition on Optical Communications (ECOC 2015), paper PDP.3.2, 2015.
[3] T. Richter, E. Palushani, C.S. Langhorst, R. Ludwig, L. Molle, M. Nölle, C. Schubert, Transmission of single-channel 16-QAM data signals at terabaud symbol rates, J. Lightw. Technol. 30 (4) (2012) 504–511.
[4] H. Zhang, C.R. Davidson, H.G. Batshon, M. Mazurczyk, Maxim Bolshtyansky, D.G. Foursa, A. Pilipetskii, DP-16QAM based coded modulation transmission in C+L band system at transoceanic distance, in Proceedings of Optical Fiber Communication Conference (OFC 2015), paper W1I.2, 2016.
[5] Z. Chen, L. Yan, Y. Pan, L. Jiang, A. Yi, W. Pan, B. Luo, Use of polarization freedom beyond polarization-division-multiplexing to support high-speed and spectral-efficient data transmission, Light Sci. & Appl. 6 (2017) 1–7.
[6] D.J. Richardson, J.M. Fini, L.E. Nelson, Space-division multiplexing in optical fibres, Nature Photon. 7 (5) (2013) 354–362.
[7] P.J. Winzer, Making spatial multiplexing a reality: the future of high-capacity optical networks, Nature Photon. 8 (5) (2014) 345–348.
[8] R.G.H. van Uden, R.A. Correa, E.A. Lopez, F.M. Huijskens, C. Xia, G. Li, A. Schülzgen, H. de Waardt, A.M.J. Koonen, C.M. Okonkwo, Ultra-high-density spatial division multiplexing with a few-mode multicore fibre, Nat. Photon., vol. advance online publication, (2014), pp. 1–6.
[9] P.J. Winzer, High-spectral-efficiency optical modulation formats, J. Lightw. Technol. 30 (24) (2012) 3824–3835.
[10] J. Wang, J.Y. Yang, I.M. Fazal, N. Ahmed, Y. Yan, H. Huang, Y. Ren, Y. Yue, S. Dolinar, M. Tur, A.E. Willner, Terabit free-space data transmission employing orbital angular momentum multiplexing, Nature Photon. 6 (2012) 488–496.
[11] D. Naidoo, F.S. Roux, A. Dudley, I. Litvin, B. Piccirillo, L. Marrucci, A. Forbes, Controlled generation of higher-order Poincare sphere beams from a laser, Nature Photon. 10 (2016) 327–333.
[12] J. Wang, Advances in communications using optical vortices, Photon. Res. 4 (5) (2016) B14–B28.
[13] A.A. Aboketaf, A.W. Elshaari, S.F. Preble, Optical time division multiplexer on silicon chip, Opt. Express 18 (13) (2010) 13529–13535.
[14] H.G. Weber, R. Ludwig, S. Ferber, C.S. Langhorst, M. Kroh, V. Marembert, C. Boerner, C. Schubert, Ultrahigh-speed OTDM-transmission technology, J. Lightw. Technol. 24 (12) (2006) 4616–4627.
[15] S. Kawanishi, H. Takara, K. Uchiyama, M. Saruwatari, T. Kitoh, Single polarization completely time-division-multiplexed 100 Gb/s optical transmission experiment, in Proceedings of European Conference and Exhibition on Optical Communications (ECOC 1993), paper 53–56, 1993.
[16] S. Weisser, S. Ferber, L. Raddatz, R. Ludwig, A. Benz, C. Boerner, H.G. Weber, Single- and alternating polarization 170 Gb/s transmission up to 4000 km using dispersion-managed fiber and all-Raman amplification, IEEE Photon. Technol. Lett. 18 (12) (2006) 1320–1322.
[17] H.G. Weber, S. Ferber, M. Kroh, C. Schmidt-Langhorst, R. Ludwig, V. Marembert, C. Boerner, F. Futami, S. Watanabe, C. Schubert, Single channel 1.28 T/s and 2.56 Tb/s DQPSK transmission, Electron. Lett. 42 (3) (2006) 178–179.

Please cite this article in press as: A. Yi, et al., Transmission of multi-dimensional signals for next generation optical communication systems, Optics Communications (2017), http://dx.doi.org/10.1016/j.optcom.2017.07.046.

[18] H. Hatakeyama, K. Naniwae, K. Kudo, N. Suzuki, S. Sudo, S. Ae, Y. Muroya, K. Yashiki, K. Satoh, T. Morimoto, K. Mori, T. Sasaki, Wavelength-selectable microarray light sources for S-, C-, and L-band WDM systems, IEEE Photon. Technol. Lett. 15 (7) (2003) 903–905.

[19] T. Matsuda, T. Kotanigawa, T. Kataoka, A. Naka, 54×42.7 Gbit/s L- and U-band WDM signal transmission experiments with in-line hybrid optical amplifiers, Electron. Lett. 40 (6) (2004) 380–381.

[20] B. Rosinski, J.W. Chi, P. Grosso, J.L. Bihan, Multichannel transmission of a multicore fiber coupled with vertical-cavity surface-emitting lasers, J. Lightw. Technol. 17 (5) (1999) 807–810.

[21] Y. Sasaki, K. Takenaga, K. Aikawa, Y. Miyamoto, T. Morioka, Single-mode 37-core fiber with a cladding diameter of 248 um, in Proceedings of Optical Fiber Communication Conference (OFC 2017), paper Th1H.2, 2017.

[22] S.K. Korotky, Price-points for components of multi-core fiber communication systems in backbone optical networks, J. Opt. Commun. Netw. 4 (5) (2012) 426–435.

[23] K. Takeshima, T. Tsuritani, Y. Tsuchida, K. Maeda, T. Saito, K. Watanabe, T. Sasa, K. Imamura, R. Sugizaki, K. Igarashi, I. Morita, M. Suzuki, 51.1 Tbit/s MCF transmission over 2520 km using cladding pumped 7-core EDFAs, in Proceedings of Optical Fiber Communication Conference (OFC 2015), paper W3G.1, 2015.

[24] B.J. Puttnam, R.S. Luís, W. Klaus, J. Sakaguchi, J.-M. Delgado Mendinueta, Y. Awaji, N. Wada, Yoshiaki Tamura, Tetsuya Hayashi, Masaaki Hirano, J. Marciante, 2.15 Pb/s transmission using a 22 core homogeneous single-mode multi-core fiber and wideband optical comb, in Proceedings of European Conference and Exhibition on Optical Communications (ECOC 2015), paper PDP.3.2, 2015.

[25] H. Takara, A. Sano, T. Kobayashi, H. Kubota, H. Kawakami, A. Matsuura, Y. Miyamoto, Y. Abe, H. Ono, K. Shikama, Y. Goto, K. Tsujikawa, Y. Sasaki, I. Ishida, K. Takenaga, S. Matsuo, K. Saitoh, M. Koshiba, T. Morioka, 1.01 Pb/s (12 SDM/222 WDM/456 Gb/s) crosstalk-managed transmission with 91.4 b/s/Hz aggregate spectral efficiency, in Proceedings of European Conference and Exhibition on Optical Communications (ECOC 2012), paper Th.3. C.1, 2012.

[26] H. Takahashi, T. Tsuritani, E.L.T. de Gabory, T. Ito, W.R. Peng, K. Igarashi, K. Takeshima, Y. Kawaguchi, I. Morita, Y. Tsuchida, Y. Mimura, K. Maeda, T. Saito, K. Watanabe, K. Imamura, R. Sugizaki, M. Suzuki, First demonstration of MC-EDFA-repeatered SDM transmission of 40 × 128 Gbit/s PDM-QPSK signals per core over 6160 km 7-core MCF, Opt. Express 21 (1) (2013) 789–795.

[27] K. Igarashi, T. Tsuritani, I. Morita, Y. Tsuchida, K. Maeda, M. Tadakuma, T. Saito, K. Watanabe, K. Imamura, R. Sugizaki, M. Suzuki, Super-Nyquist-WDM transmission over 7326 km seven-core fiber with capacity-distance product of 1.03 Exabit/s·km, Opt. Express 22 (2) (2014) 1220–1228.

[28] A. Turukhin, O.V. Sinkin, H.G. Batshon, H. Zhang, Y. Sun, M. Mazurczyk, C.R. Davidson, J.-X. Cai, M.A. Bolshtyansky, D.G. Foursa, A. Pilipetskii, 105.1 Tb/s power-efficient transmission over 14,350 km using a 12-core fiber, in Proceedings of Optical Fiber Communication Conference (OFC 2016), paper Th4C.1, 2016.

[29] T. Mizuno, K. Shibahara, H. Ono, Y. Abe, Y. Miyamoto, F. Ye, T. Morioka, Y. Sasaki, Y. Amma, K. Takenaga, S. Matsuo, K. Aikawa, K. Saitoh, Y. Jung, D.J. Richardson, K. Pulverer, M. Bohn, M. Yamada, 32-core dense SDM unidirectional transmission of PDM-16QAM signals over 1600 km using crosstalk-managed single-mode heterogeneous multicore transmission line, in Proceedings of Optical Fiber Communication Conference (OFC 2016), paper Th5C.3, 2016.

[30] T. Kobayashi, M. Nakamura, F. Hamaoka, K. Shibahara, T. Mizuno, A. Sano, H. Kawakami, A. Isoda, M. Nagatani, H. Yamazaki, Y. Miyamoto, Y. Amma, Y. Sasaki, K. Takenaga, K. Aikawa, K. Saitoh, Y. Jung, D.J. Richardson, K. Pulverer, M. Bohn, M. Nooruzzaman, T. Morioka, 1 Pb/s (32 SDM/46 WDM/768 Gb/s) C-band dense SDM transmission over 205.6 km of single-mode heterogeneous multi-core fiber using 96 Gbaud PDM-16QAM channels, in Proceedings of Optical Fiber Communication Conference (OFC 2017), paper Th5B.1, 2017.

[31] R.G.H. Uden, C.M. Okonkwo, V.A.J.M. Sleiffer, H. de Waardt, A.M.J. Koonen, MIMO equalization with adaptive step size for few-mode fiber transmission, Opt. Express 22 (1) (2014) 119–126.

[32] P. Sillard, D. Molin, M. Bigot-Astruc, K. de Jongh, F. Achten, J.E. Antonio-López, R. Amezcua-Correa, Low-DMGD 6-LP-mode fiber. in processing of Optical Fiber Communication Conference (OFC2014), paper M3F.2, 2014.

[33] P. Sillard, D. Molin, M. Bigot-Astruc, K. de Jongh, F. Achten, J.E. Antonio-López, R. Amezcua-Correa, Micro-bend-resistant low-differential-mode-group-delay few-mode fibers, J. Lightw. Technol. 35 (4) (2017) 734–740.

[34] E. Ip, M.J. Li, K. Bennett, Y.K. Huang, A. Tanaka, A. Korolev, K. Koreshkov, W. Wood, E. Mateo, J. Hu, Y. Yano, 146λ × 6 × 19 Gbaud wavelength and mode-division multiplexed transmission over 10 × 50 km spans of few-mode fiber with a gain-equalized few-mode EDFA, J. Lightw. Technol. 32 (4) (2014) 790–797.

[35] R. Ryf, N.K. Fontaine, H. Chen, B. Guan, B. Huang, M. Esmaeelpour, A.H. Gnauck, S. Randel, S.J.B. Yoo, A.M.J. Koonen, R. Shubochkin, Y. Sun, R. Lingle, Mode-multiplexed transmission over conventional graded-index multimode fibers, Opt. Express 23 (1) (2015) 235–246.

[36] Y. Chen, A. Lobato, Y. Jung, H. Chen, V.A.J.M. Sleiffer, M. Kuschnerov, N.K. Fontaine, R. Ryf, D.J. Richardson, B. Lank, N. Hanik, 41.6 Tbit/s C-Band SDM OFDM transmission through 12 spatial and polarization modes over 74.17 km few mode fiber, J. Lightw. Technol. 33 (7) (2015) 1440–1444.

[37] R. Ryf, S. Randel, N.K. Fontaine, M. Montoliu, E. Burrows, S. Corteselli, S. Chandrasekhar, A.H. Gnauck, C. Xie, R.-J. Essiambre, P.J. Winzer, R. Delbue, P. Pupalaikis, A. Sureka, Y. Sun, L.G. Nielsen, R.V. Jensen, R. Lingle, 32 bit/s/Hz spectral efficiency WDM transmission over 177 km few-mode fiber, in Proceedings of Optical Fiber Communication Conference (OFC 2013), paper PDP5A.1, 2013.

[38] R. Ryf, S. Randel, N.K. Fontaine, X. Palou, E. Burrows, S. Corteselli, S. Chandrasekhar, A.H. Gnauck, C. Xie, R.-J. Essiambre, P.J. Winzer, R. Delbue, P. Pupalaikis, A. Sureka, Y. Sun, L.G. Nielsen, R.V. Jensen, R. Lingle, 708 km combined WDM/SDM transmission over few-mode fiber supporting 12 spatial and polarization modes, in Proceedings of Optical Fiber Communication Conference (OFC 2013), paper We.2. D.1, 2013.

[39] R. Ryf, N.K. Fontaine, M. Montoliu, S. Randel, B. Ercan, H. Chen, S. Chandrasekhar, A.H. Gnauck, S.G. Leon-Saval, J. Bland-Hawthorn, J.R. Salazar-Gil, Y. Sun, R. Lingle, Photonic-lantern-based mode multiplexers for few-mode-fiber transmission, in Proceedings of Optical Fiber Communication Conference (OFC 2014), paper W4J.2, 2014.

[40] N.K. Fontaine, R. Ryf, H. Chen, A.V. Benitez, J.E.A. Lopez, R.A. Correa, B. Guan, B. Ercan, R.P. Scott, S.J.B. Yoo, L.G. Nielsen, Y. Sun, R.J. Lingle, 30 × 30 MIMO transmission over 15 spatial modes, in Proceedings of Optical Fiber Communication Conference (OFC 2015), paper Th5C.1, 2015.

[41] J.J.A. van Weerdenburg, A.M. Velazquez Benitez, R.G.H. van Uden, J.E. Antonio-Lopez, P. Sillard, D. Molin, M. Bigot-Astruc, A. Amezcua-Correa, F.M. Huijskens, F. Achten, H. de Waardt, A.M.J. Koonen, R. Amezcua-Correa, C.M. Okonkwo, 10 Spatial mode transmission over 40 km 50 μm core diameter multimode fiber, in Proceedings of Optical Fiber Communication Conference (OFC 2016), paper Th4C.3, 2016.

[42] H. Chen, R. Ryf, N.K. Fontaine, A.M. Velázquez-Benítez, José Antonio-López, C. Jin, B. Huang, M. Bigot-Astruc, D. Molin, F. Achten, P. Sillard, R. Amezcua-Correa, High spectral efficiency mode-multiplexed transmission over 87 km 10-mode fiber, in Proceedings of Optical Fiber Communication Conference (OFC 2016), paper Th4C.2, 2016.

[43] C. Xia, R.A. Correa, N. Bai, E.A. Lopez, D.M. Arrioja, A. Schulzgen, M. Richardson, J. Linares, C. Montero, E. Mateo, X. Zhou, G. Li, Hole-assisted few-mode multicore fiber for high-density space-division multiplexing, IEEE Photon. Technol. Lett. 24 (21) (2012) 1914–1916.

[44] Y. Sasaki, K. Takenaga, N. Guan, S. Matsuo, K. Saitoh, M. Koshiba, Large-effective-area uncoupled few-mode multi-core fiber, in Proceedings of the European Conference on Optical Communication (ECOC 2012), paper Tu.1. F.3, 2012.

[45] T. Mizuno, H. Takara, A. Sano, H. Kawakami, D. Lee, Y. Miyamoto, H. Ono, M. Oguma, Y. Abe, T. Kobayashi, T. Matsui, R. Fukumoto, Y. Amma, T. Hosokawa, S. Matsuo, K. Saito, H. Nasu, T. Morioka, Dense SDM (12-core × 3-mode) transmission over 527 km with 33.2 ns mode dispersion employing low complexity parallel MIMO frequency domain equalization, in Proceedings of Optical Fiber Communication Conference (OFC 2015), paper Th5C.3, 2015.

[46] D. Soma, Y. Wakayama, S. Beppu, K. Igarashi, T. Tsuritani, H. Taga, I. Morita, M. Suzuki, 665 and 947/b/s/Hz ultra-highly aggregate-spectral-efficient SDM/WDM transmission over 6-mode 19-core fibre using DP-16QAM/64QAM signals, in Proceedings of the European Conference on Optical Communication (ECOC 2016), paper PDP 37–39, 2016.

[47] Y. Wang, K. Kasai, M. Yoshida, M. Nakazawa, Single-carrier 216 Gbit/s, 12 Gsymbol/s 512 QAM coherent transmission over 160 km with injection-locked homodyne detection, in Proceedings of Optical Fiber Communication Conference (OFC 2017), paper Tu2E.1, 2017.

[48] Y. Wang, K. Kasai, M. Yoshida, M. Nakazawa, 320 Gbit/s, 20 Gsymbol/s 256 QAM coherent transmission over 160 km by using injection locked local oscillator, Opt. Express 24 (19) (2016) 22088–22096.

[49] G. Khanna, T. Rahman, E. Man, E. Riccardi, A. Pagano, A. Piat, S. Calabrò, B. Spinnler, D. Rafique, U. Feiste, H. Waardt, B. Krombholz, N. Hanik, T. Drenski, M. Bohn, A. Napoli, Single-carrier 400 G 64QAM and 128QAM DWDM field trial transmission over metro legacy links, IEEE Photon. Technol. Lett. 29 (2) (2017) 189–192.

[50] K. Schuh, F. Buchali, W. Idler, T. Eriksson, L. Schmalen, W. Templ, L. Altenhain, U. Dümler, R. Schmid, M. Möller, K. Engenhardt, Single carrier 1.2 Tbit/s transmission over 300 km with PM-64 QAM at 100 GBaud, in Proceedings of Optical Fiber Communication Conference (OFC 2017), paper Th5B.5, 2017.

[51] R. Rios-Müller, J. Renaudier, P. Brindel, H. Mardoyan, P. Jennevé, L. Schmalen, G. Charlet, 1 Terabit/s net data-rate transceiver based on single-carrier Nyquist-shaped 124 GBaud PDM-32QAM, in Proceedings of Optical Fiber Communication Conference (OFC 2015), paper Th5B.1, 2015.

[52] A. Matsushita, F. Hamaoka, M. Nakamura, K. Horikoshi, H. Yamazaki, M. Nagatani, A. Sano, A. Hirano, Y. Miyamoto, Super-Nyquist 9-WDM 126 GBaud PDM-QPSK transmission over 7878 km using digital-preprocessed analog-multiplexed DAC for long-haul applications, in Proceedings of European Conference on Optical Communications (ECOC 2016), paper 671–673, 2016.

[53] S. Beppu, K. Kasai, M. Yoshida, M. Nakazawa, 2048 QAM (66 Gbit/s) single-carrier coherent optical transmission over 150 km with a potential SE of 15.3 bit/s/Hz, Opt. Express 23 (4) (2015) 11590–11605.

[54] J. Cai, Y. Sun, H. Batshon, M. Mazurczyk, H. Zhang, D. Foursa, A. Pilipetskii, 54 Tb/s transmission over 9150 km with optimized hybrid Raman-EDFA amplification and coded modulation, in Proceedings of European Conference on Optical Communications (ECOC 2014), paper PD.3.3, 2014.

[55] J. Cai, H. Batshon, M. Mazurczyk, H. Zhang, Y. Sun, O. Sinkin, D. Foursa, A. Pilipetskii, 64QAM based coded modulation transmission over transoceanic distance with >60 Tb/s capacity, in Proceedings of Optical Fiber Communication Conference (OFC 2015), paper Th5C.8, 2015.

Please cite this article in press as: A. Yi, et al., Transmission of multi-dimensional signals for next generation optical communication systems, Optics Communications (2017), http://dx.doi.org/10.1016/j.optcom.2017.07.046.

[56] S. Zhang, F. Yaman, Y. Huang, J. Downie, D. Zou, W. Wood, A. Zakharian, R. Khrapko, S. Mishra, V. Nazarov, J. Hurley, I. Djordjevic, E. Mateo, Y. Inada, Capacity-approaching transmission over 6375 km at spectral efficiency of 8.3 bit/s/Hz, in Proceedings of Optical Fiber Communication Conference (OFC 2016), paper Th5C.2, 2016.

[57] L. Mandel, E. Wolf, Optical Coherence and Quantum Optics, Cambridge Univ. Press, 1995.

[58] M. Padgett, R. Bowman, Tweezers with a Twist, Nature Photon. 5 (2011) 343–348.

[59] M.R. Dennis, R.P. King, B. Jack, K. O'Holleran, M.J. Padgett, Isolated optical vortex knots, Nat. Phys. 6 (2010) 118–121.

[60] J. Leach, B. Jack, J. Romero, A. Jha, A.M. Yao, S.F. Arnold, D.G. Ireland, R.W. Boyd, S.M. Barnett, M.J. Padgett, Quantum correlations in optical angle-orbital angular momentum variables, Science 329 (2010) 662–665.

[61] G. Gibson, J. Courtial, Miles J. Padgett, Free-space information transfer using light beams carrying orbital angular momentum, Opt. Express 12 (22) (2004) 5448–5456.

[62] N. Bozinovic, Y. Yue, Y. Ren, M. Tur, P. Kristensen, H. Huang, A.E. Willner, S. Ramachandran, Terabit-scale orbital angular momentum mode division multiplexing in fibers, Science 340 (2013) 1545–1548.

[63] L. Zhu, A. Wang, S. Chen, J. Liu, C. Du, Q. Mo, J. Wang, Experimental demonstration of orbital angular momentum (OAM) modes transmission in a 2.6 km conventional graded-index multimode fiber assisted by high efficient mode-group excitation, in Proceedings of Optical Fiber Communication Conference (OFC 2016), paper W2A.32, 2016.

[64] F. Feng, X. Jin, D. O'Brien, F.P. Payne, T.D. Wilkinson, Mode-group multiplexed transmission using OAM modes over 1 km ring-core fiber without MIMO processing, in Proceedings of Optical Fiber Communication Conference (OFC 2017), paper Th2A.43, 2017.

[65] K. Ingerslev, P. Gregg, M. Galili, F. Da Ros, H. Hu, F. Bao, M.A.U. Castaneda, P. Kristensen, A. Rubano, L. Marrucci, S. Ramachandran, K. Rottwitt, T. Morioka, L.K. Oxenløwe, 12 Mode, MIMO-free OAM transmission, in Proceedings of Optical Fiber Communication Conference (OFC 2017), paper M2D.1, 2017.

[66] G. Milione, T. Nguyen, J. Leach, D.A. Nolan, R.R. Alfano, Using the nonseparability of vector beams to encode information for optical communication, Opt. Lett. 40 (21) (2015) 4887–4890.

[67] G. Milione, M.P.J. Lavery, H. Huang, Y. Ren, G. Xie, T. Nguyen, E. Karimi, L. Maccrucci, D.A. Nolan, R.R. Alfano, A.E. Willner, 4 × 20 Gbit/s mode division multiplexing over free space using vector modes and a q-plate mode (de)multiplexer, Opt. Let. 40 (9) (2015) 1980–1983.

[68] J. Zhang, F. Li, J. Li, Y. Feng, Z. Li, 120 Gbit/s 2 × 2 Vector-modes-division-multiplexing DD-OFDM-32QAM free-space transmission, IEEE Photon. Journal 8 (6) (2016) 7907008 (1)–(9).

[69] J. Zhang, F. Li, J. Li, Z. Li, 95.16 Gb/s Mode-division-multiplexing signal transmission in free-space enabled by effective-conversion of vector beams, IEEE Photon. Journal 9 (4) (2017) 7202809(1)–(10).

[70] B. Ndagno, R. Bruning, M. McLaren, M. Duparrre, A. Forbes, Fiber propagation of vector modes, Opt. Express 23 (13) (2015) 17330–17336.

[71] S. Ramachandran, P. Kristensen, M.F. Yan, Generation and propagation of radially polarized beams in optical fibers, Optics Let. 34 (16) (2009) 2525–2527.

[72] Y. Han, G. Li, Coherent optical communication using polarization multiple-input-multiple-output, Opt. Express 13 (19) (2005) 7527–7534.

[73] Mollenauer, L.F. S. G. Evangelides Jr., J.P. Gordon, N.S. Bergano, Polarization multiplexing with solitons, J. Lightw. Technol. 10 (1) (1992) 28–35.

[74] W. Shieh, X. Yi, Y. Ma, Y. Tang, Theoretical and experimental study on PMD-supported transmission using polarization diversity in coherent optical OFDM system, Opt. Express 15 (16) (2007) 9936–9947.

[75] P.J. Winzer, A.H. Gnauck, 112 Gb/s polarization-multiplexed 16-QAM on a 25 GHz WDM grid, in Proceeding of European Conference on Optical Communication (ECOC'2008), paper Th.3. E.5, 2008.

[76] X. Zhou, J.J. Yu, M.F. Huang, Y. Shao, T. Wang, P. Magill, M. Cvijetic, L. Nelson, M. Birk, G.D. Zhang, S.Y. Ten, H.B. Matthew, S.K. Mishra, 32 Tb/s (320 × 114Gb/s) PDM-RZ-8QAM transmission over 580 km of SMF-28 ultra-low-loss fiber, in proceeding of Optical Fiber Communication (OFC 2009), paper PDPB4, 2009.

[77] D.Y. Qian, M.F. Huang, E. Ip, Y.K. Huang, Y. Shao, J.Q. Hu, T. Wang, 101.7 Tb/s (370-294 Gb/s) PDM-128QAM-OFDM transmission over 3 × 55 km SSMF using pilot-based phase noise mitigation, in proceeding of Optical Fiber Communication (OFC 2011), paper PDPB5, 2011.

[78] X. Liu, S. Chandrasekhar, X. Chen, P.J. Winzer, Y. Pan, T.F. Taunay, B. Zhu, M. Fishteyn, M.F. Yan, J.M. Fini, E.M. Monberg, F.V. Dimarcello, 1.12 Tb/s 32-QAM-OFDM superchannel with 8.6 b/s/Hz intrachannel spectral efficiency and space-division multiplexed transmission with 60 b/s/Hz aggregate spectral efficiency, Opt. Express 19 (26) (2011) B958–B964.

[79] C.R.S. Fludger, T. Duthel, D. van den Borne, C. Schulien, E.D. Schmidt, T. Wuth, J. Geyer, E.D. Man, G.D. Khoe, H. de Waardt, Coherent equalization and POLMUX-RZ-DQPSK for robust 100 GE transmission, J. Lightw. Technol. 26 (1) (2008) 64–72.

[80] C. Herard, A. Lacourt, Three channel multiplexing using polarization of light, Opt. Commun. 60 (1) (1986) 27–31.

[81] Z. Chen, L. Yan, W. Pan, B. Luo, Y. Guo, H. Jiang, A. Yi, Y. Sun, X. Wu, Transmission of multi-polarization-multiplexed signals: another freedom to explore? Opt. Express 21 (9) (2013) 11590–11605.

[82] J. Estarán, M.A. Usuga, E. Porto, M. Piels, M.I. Olmedo, I. Tafur Monroy, Quad-polarization transmission for high-IM/DD links, in Proceedings of the European Conference on Optical Communication (ECOC 2014), paper PD.4.3, 2014.

[83] B. Szafraniec, B. Nebendahl, T. Marshall, Polarization demultiplexing in stokes space, Opt. Express 18 (17) (2010) 17928–17939.

[84] L. Jiang, L. Yan, A. Yi, Z. Chen, Y. Pan, W. Pan, B. Luo, X. Zhou, X. Feng, Minimizing polarization multiplexing angle in polarization-division-multiplexed system, Photon. J. 8 (2) (2016) 1–8.

[85] Y. Pan, L. Yan, A. Yi, Z. Chen, L. Jiang, W. Pan, B. Luo, X. Zou, X. Zhou, X. Feng, Transmission of three-polarization-multiplexed 25 Gb/s DPSK signals over 300 km fiber link, Opt. Lett. 41 (7) (2016) 1620–1623.

Please cite this article in press as: A. Yi, et al., Transmission of multi-dimensional signals for next generation optical communication systems, Optics Communications (2017), http://dx.doi.org/10.1016/j.optcom.2017.07.046.